A missing data method for deconfounding in neuroimaging studies

Benjamin Risk

Department of Biostatistics & Bioinformatics,
Rollins School of Public Health, Emory University

11 October 2021

Based on the working manuscript

Accounting for motion in fMRI: What part of the spectrum are we characterizing in autism?

Mary Beth Nebel[1], Daniel Lidstone[1], Liwei Wang[2], Stewart Mostofsky[1], David Benkeser[2], and Benjamin Risk[2]

[1]Kennedy Krieger Institute and Johns Hopkins University School of Medicine
[2]Department of Biostatistics & Bioinformatics, Emory University

Functional connectivity and resting-state fMRI

- Functional connectivity: spontaneous correlations between brain regions.
- Resting-state fMRI scans from Kennedy Krieger Institute and JHU SOM (either 5:20 or 6:45 seconds in length).
- Children are asked to remain motionless while staring at crosshairs.
- This is challenging, particularly for children with autism.
- Motion in the scanner produces artifacts.

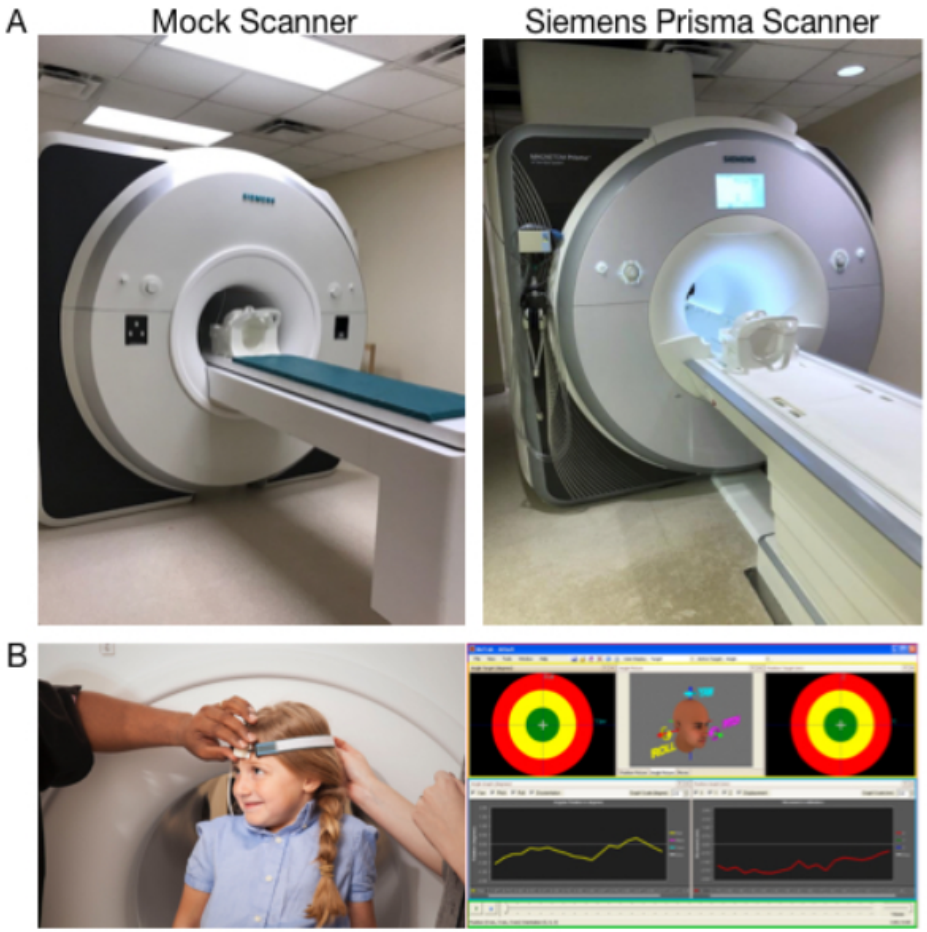

Motion quality control exclusion

- Goal: $E[Y|A=1] - E[Y|A=0]$.
- Connectivity hypothesis of autism: short-range connections increased at the expense of long-range connections (Deen and Pelphrey, 2012; Just et al., 2004).
- Motion looks like an increase in short- and decrease in long-range (Power et al., 2012).
- Lenient: < 5 min data after removing frames > 3 mm or $3°$ from previous frame (Fassbender et al., 2017).
- Strict: mean framewise displacement $> .2$ mm or < 5 min data after excluding FD $> .25$ mm (Ciric et al., 2017).

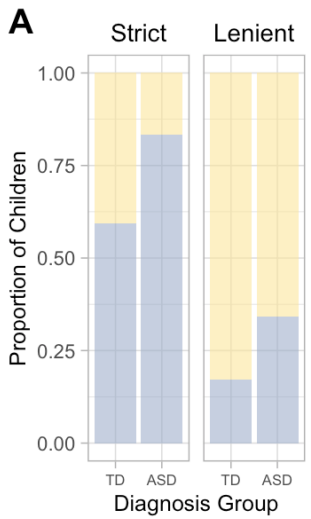

Figure: Quality control removes 30-83% of children with ASD and 12-60% of typically developing.

The problem: motion exclusion criteria causes sampling bias

- Motion quality control reduces one problem but creates a new problem: sample bias.

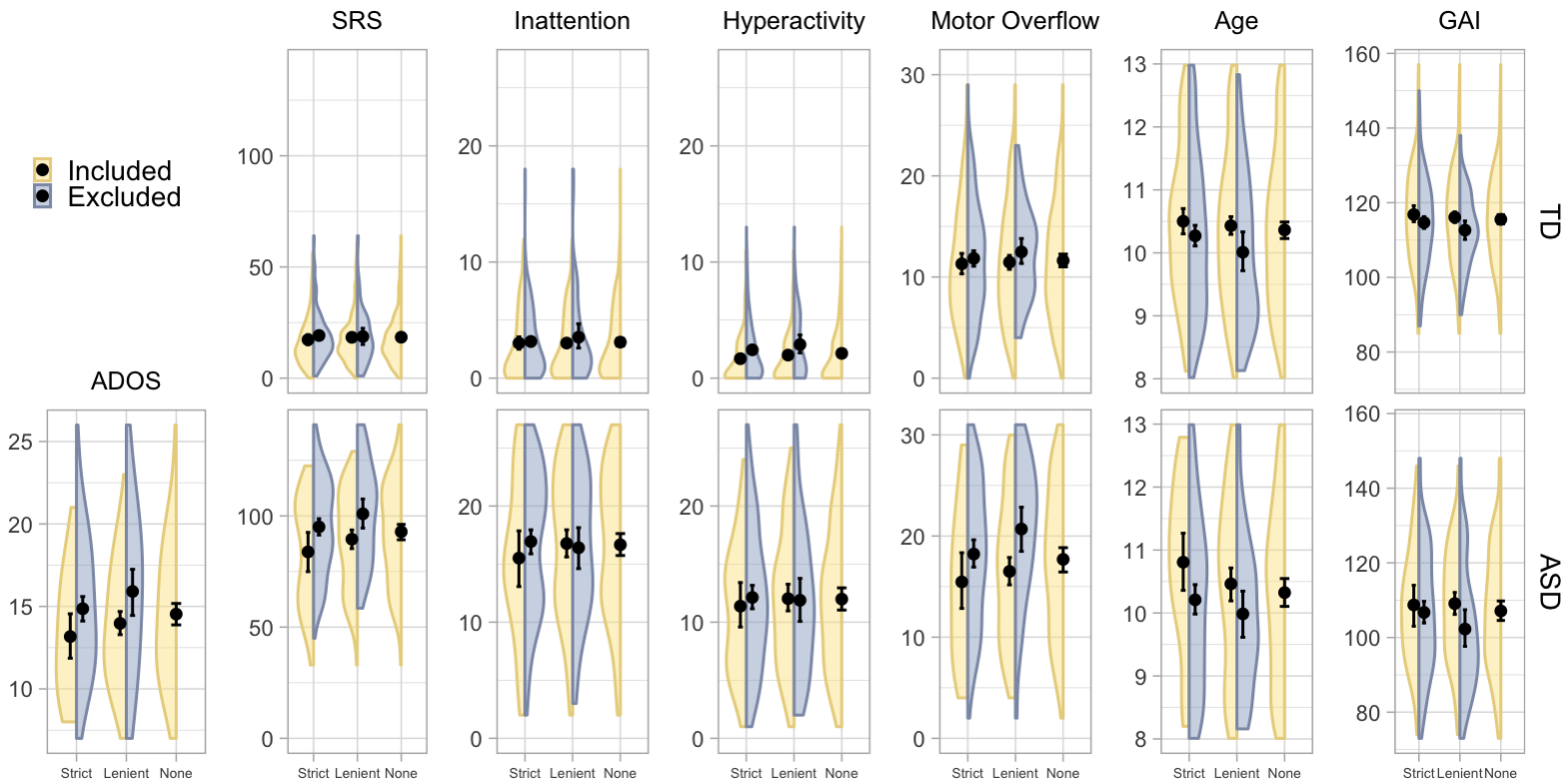

Figure: During QC, **more severe cases of autism are excluded.**

The problem: some behavioral measures are related to functional connectivity.

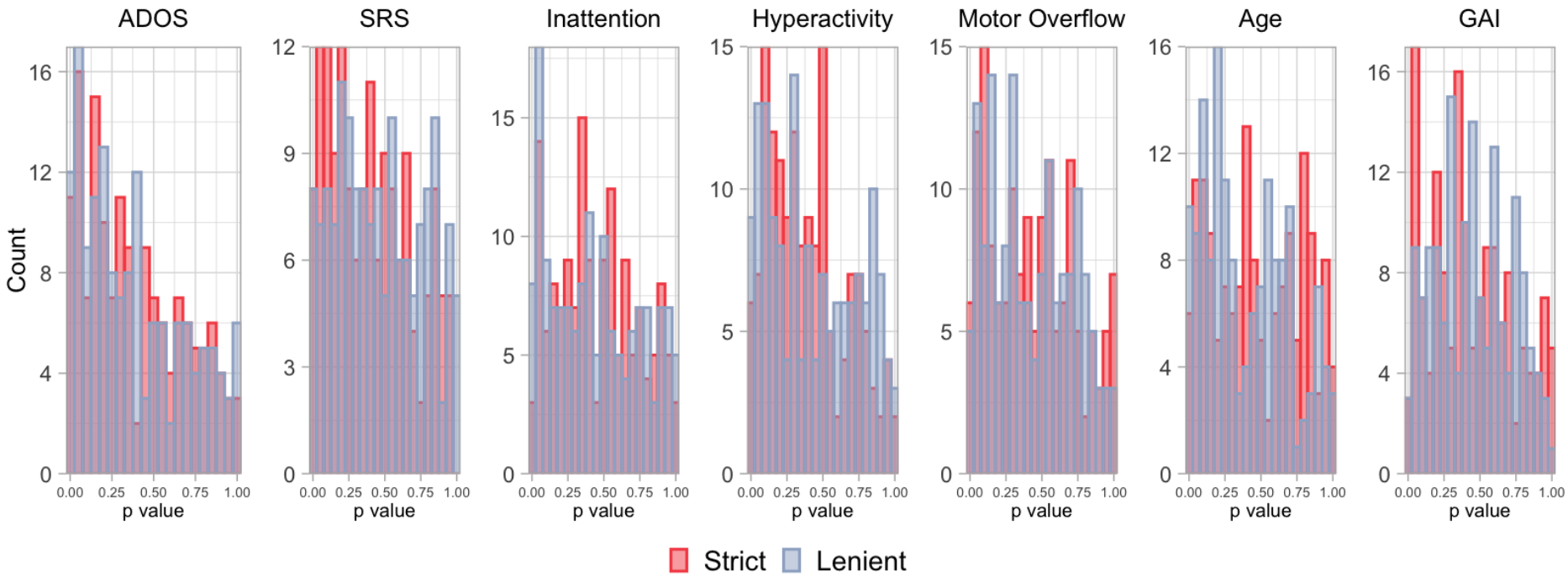

Figure: **Some covariates related to rs-fMRI exclusion probability are also related to functional connectivity**. Histograms of p-values from univariate GAMs at 153 brain connections.

The problem: confounding due to motion exclusion

- $Y(1)$ is the counterfactual that a participant's scan is usable; A is diagnosis; W are behavioral measures.
- Define a novel parameter of interest:

$$\psi^* = E^* \left\{ E^* \left(Y(1) | A = 1, W \right) | \, A = 1 \right\} \\ - E^* \left\{ E^* \left(Y(1) | A = 0, W \right) | A = 0 \right\}$$

- The naïve estimator:

$$\psi_{naive} = E \left\{ E \left(Y | \Delta = 1, A = 1, W \right) | \, \Delta = 1, A = 1 \right\} \\ - E \left\{ E \left(Y(1) | \Delta = 1, A = 0, W \right) | \Delta = 1, A = 0 \right\}$$

- Confounding: $\psi_{naive} \neq \psi^*$, e.g., Greenland et al. (1999).

The solution: Deconfounded group difference

- $\Delta = 0$ (unusable data) are treated as missing data.
- We define the target parameter, which we call the **deconfounded group difference**:

$$\psi = E\{E(Y \mid \Delta = 1, A = 1, W) \mid A = 1\} - E\{E(Y \mid \Delta = 1, A = 0, W) \mid A = 0\}.$$

- $\psi = \psi^*$ under assumptions:
  - (A1.1) *Conditional Randomization*: for $a = 0, 1$,

$$E^*\{Y(1) \mid A = a, W\} = E\{Y \mid \Delta = 1, A = a, W\}.$$

  - (A1.2) *Positivity*: for $a = 0,\ 1$ and all possible w,

$$P(\Delta = 1 \mid A = a, W = w) > 0.$$

  - (A1.3) *Consistency*: for all i such that $\Delta_i = 1$, $Y_i(1) = Y_i$,

Deconfounded group difference

- Consider group specific targets: $\psi_{A=1}$ and $\psi_{A=0}$.
- Propensity model:

$$g(a, w) = P(\Delta = 1 | A = a, W = w)$$

- Classic IPW. For $a_i = 1$,

$$\hat{\psi}_{IPW,A=1} = \mathbb{E}_{n,a=1} \left\{ \frac{I(\Delta_i = 1)}{g_n(a_i = 1, w_i)} y_i \right\}$$

- Outcome model:

$$\bar{Q}(a, w) = E(Y | \Delta = 1, A = a, W = w)$$

- Classic G-computation estimator:

$$\hat{\psi}_{G,A=1} = \mathbb{E}_{n,a=1} \left\{ \bar{Q}_n(\Delta = 1, a_i = 1, w_i) \right\}$$

Doubly robust targeted minimum loss based estimation

- Use ensemble of machine learning methods to fit the propensity and outcome models (Van Der Laan et al., 2007).
- Estimate using doubly robust targeted minimum loss based estimation.
- DRTMLE from Benkeser et al. (2017) combines propensity and outcome models in a manner that
  - is efficient when both outcome and propensity models are consistent;
  - is consistent when at least one of the outcome or propensity models is consistent;
  - asymptotically normal with a variance that is consistent if at least one of the outcome or propensity models is consistent.

Data Analysis: Functional connectivity

- Resting-state fMRI scans from Kennedy Krieger Institute (either 5:20 or 6:45 seconds in length).
- 151 ASD children and 353 typically developing.
- Used lenient criteria.
- 107 ASD and 296 TD pass lenient criteria.
- Defined a "parcellation" using group ICA via GIFT with 30 components (Calhoun et al., 2001).
- Resulted in a time course for 30 components.
- Calculated partial correlation matrix for each child.
- Identified 18 signal components, looked at 153 partial correlations = functional connectivity.
- FConn processing follows a recent study of ASD in toddlers (Lombardo et al., 2019).

Data Analysis: Propensity and outcome models

- Input to drtmle: for each edge, residuals from a linear regression of functional connectivity vs motion variables, race, SES, sex, and dx with dx added back in.
- SuperLearner with 10-fold CV for propensity and outcome models: `SL.earth`, `SL.glmnet`, `SL.gam`, `SL.glm`, `SL.ranger`, `SL.ridge`, `SL.step`, `SL.step.interaction`, `SL.svm`, `SL.xgboost`.
- Predictors: `Primary diagnosis`, `Head coil`, `ADHD secondary`, `Age at scan`, `Handedness`, `Stimulants`, `Motor overflow`, `General ability index`, `Inattention`, `Hyperactivity`, `Autism diagnostic observation schedule`.

Results

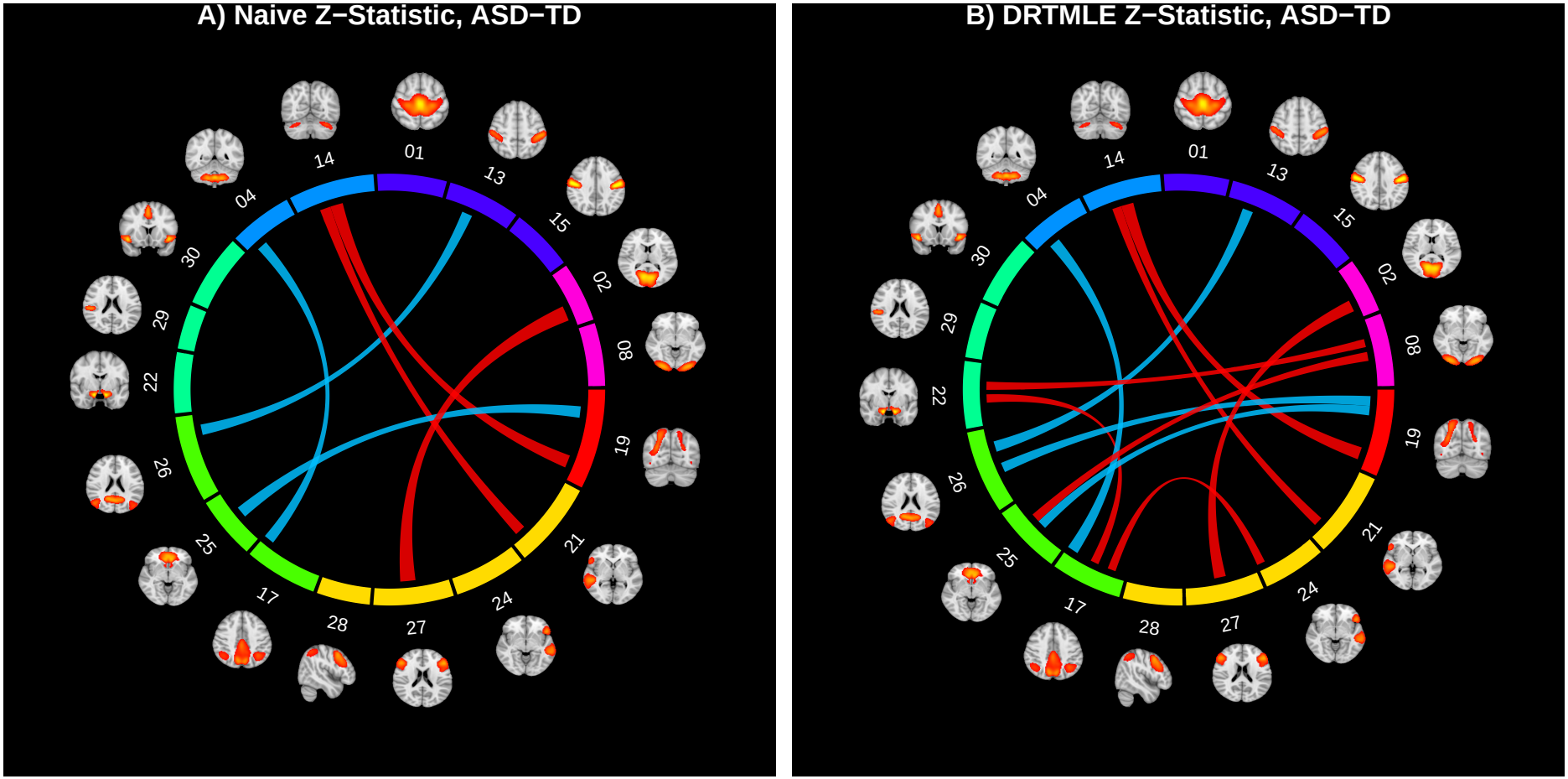

Figure: **The deconfounded group difference via DRTMLE reveals more extensive differences** between ASD and TD. Z-stats from partial correlations from the group ICA parcellation. Thresholded at FDR=0.20. Blue: ASD>TD. Naive: 6 edges, DRTMLE: 11 edges.

Discussion

- Participant exclusion due to motion quality control creates large sampling biases.
- We use DRTMLE to estimate the deconfounded group difference in a large study of autism spectrum disorder.
- More extensive differences between ASD and TD when accounting for sampling biases via DRTMLE.
- Future directions: develop estimator allowing for covariates that we balance between groups (demographics such as race, SES, sex) versus covariates for which we condition on diagnosis (measures of autism severity).
- Improved inference for finite samples.
- Additional info: `https://github.com/thebrisklab/DeconfoundedFMRI`
- Thank you!

References I

Benkeser, D., Carone, M., Laan, M. J. V. D., and Gilbert, P. B. (2017). Doubly robust nonparametric inference on the average treatment effect. *Biometrika*, 104(4):863–880.

Calhoun, V. D., Adali, T., Pearlson, G. D., and Pekar, J. J. (2001). A method for making group inferences from functional MRI data using independent component analysis. *Human Brain Mapping*, 14(3):140–151.

Ciric, R., Wolf, D. H., Power, J. D., Roalf, D. R., Baum, G. L., Ruparel, K., Shinohara, R. T., Elliott, M. A., Eickhoff, S. B., Davatzikos, C., Gur, R. C., Gur, R. E., Bassett, D. S., and Satterthwaite, T. D. (2017). Benchmarking of participant-level confound regression strategies for the control of motion artifact in studies of functional connectivity. *NeuroImage*, 154:174–187.

Deen, B. and Pelphrey, K. (2012). Perspective: Brain scans need a rethink.

Fassbender, C., Mukherjee, P., and Schweitzer, J. B. (2017). Reprint of: Minimizing noise in pediatric task-based functional MRI; Adolescents with developmental disabilities and typical development. *NeuroImage*, 154:230–239.

Greenland, S., Robins, J. M., and Pearl, J. (1999). Confounding and collapsibility in causal inference. *Statistical Science*, 14(1).

References II

Just, M. A., Cherkassky, V. L., Keller, T. A., and Minshew, N. J. (2004). Cortical activation and synchronization during sentence comprehension in high-functioning autism: Evidence of underconnectivity. *Brain*, 127(8):1811–1821.

Lombardo, M. V., Eyler, L., Moore, A., Datko, M., Barnes, C. C., Cha, D., Courchesne, E., and Pierce, K. (2019). Default mode-visual network hypoconnectivity in an autism subtype with pronounced social visual engagement difficulties. *eLife*, 8:e47427–undefined.

Power, J. D., Barnes, K. A., Snyder, A. Z., Schlaggar, B. L., and Petersen, S. E. (2012). Spurious but systematic correlations in functional connectivity MRI networks arise from subject motion. *NeuroImage*, 59(3):2142–2154.

Van Der Laan, M. J., Polley, E. C., and Hubbard, A. E. (2007). Super learner. *Statistical Applications in Genetics and Molecular Biology*, 6(1).